Construction of exact simultaneous confidence bands for a simple linear regression model

W. Liu and S. Lin

S^3RI and School of Mathematics

University of Southampton, Southampton SO17 1BJ, UK

W.Liu@maths.soton.ac.uk, S.Lin@soton.ac.uk

W.W. Piegorsch

Department of Mathematics

The University of Arizona, AZ 85721, USA

piegorsch@math.arizona.edu

1st version October 2006, revision September 2007

Summary

A simultaneous confidence band provides a variety of inferences on the unknown components of a regression model. There are several recent papers using confidence bands for various inferential purposes; see for example Sun, Raz and Faraway (1999), Spurrier (1999), Al-Saidy et al. (2003), Liu, Jamshidian and Zhang (2004), Bhargava and Spurrier (2004), Piegorsch et al. (2005), and Liu et al. (2007). Construction of simultaneous confidence bands for a simple linear regression model has a rich history, going back to the work of Working and Hotelling (1929). The purpose of this article is to consolidate the disparate modern literature on simultaneous confidence bands in linear regression, and to provide expressions for the construction of exact $1-\alpha$ level simultaneous confidence bands for a simple linear regression model of either one-sided or two-sided form. We center attention on the three most recognized shapes: hyperbolic, two-segment, and three-segment (which is also referred to as a trapezoidal shape and includes a constant-width band as a special case). Some of these expressions have already appeared in the statistics literature, and some are newly derived in this article. The derivations typically involve a standard bivariate t random vector and its polar coordinate transformation.

Key words: Simple linear regression; Simultaneous inferences; Bivariate normal; Bivariate t; Polar coordinators.

1 Introduction

Suppose that data (x_j, y_j) are available which are modelled as

$$y_j = b_0 + b_1 x_j + \epsilon_j$$

for $1 \le j \le n$, where the ϵ_j are independently distributed as $N(0, \sigma^2)$ random variables, and b_0, b_1 and σ^2 are unknown parameters.

Let X denote the design matrix, whose ith row is given by $(1, x_i), i = 1, \cdots, n$. Then

$$(X^T X)^{-1} = \frac{1}{\sum_{j=1}^{n}(x_j - \bar{x})^2} \begin{pmatrix} \sum_{j=1}^{n} x_j^2/n, & -\bar{x} \\ -\bar{x}, & 1 \end{pmatrix}$$

where $\bar{x} = \sum_{j=1}^{n} x_j/n$. Denote the least square estimators of $\mathbf{b} = (b_0, b_1)^T$ and σ by $\hat{\boldsymbol{b}} = (\hat{b}_0, \hat{b}_1)^T$ and $\hat{\sigma}$ respectively. Then $\hat{\boldsymbol{b}} \sim N_2(\mathbf{b}, \sigma^2 (X^T X)^{-1})$, $\hat{\sigma}/\sigma \sim \sqrt{\chi_k^2/k}$ where $k = n-2$, and $\hat{\boldsymbol{b}}$ and $\hat{\sigma}$ are independent random variables.

In this article we consider the construction of confidence bands $(l(x), u(x))$ for $b_0 + b_1 x$ over an interval $x \in (a, A)$ that have simultaneous confidence level equal to $1 - \alpha$:

$$\inf_{-\infty < b_0, b_1 < \infty,\ \sigma > 0} \mathrm{P}\{\ l(x) < b_0 + b_1 x < u(x)\ \text{ for all } x \in (a, A)\ \} = 1 - \alpha \tag{1}$$

where $l(x)$ and $u(x)$ are given functions representing the lower and upper components respectively of the band, with $-\infty \le a < A \le \infty$ and $\alpha \in (0, 1)$ as given constants. A confidence band provides useful information on where the true but unknown regression line lies; a straight line is a plausible candidate for the unknown regression line if and only if it is contained completely inside the confidence band. There are several recent papers that consider applications of confidence bands. For example, Sun, Raz and Faraway (1999) used simultaneous confidence bands for making inferences about growth and response curves, Al-Saidy *et al.* (2003) and Piegorsch *et al.* (2005) used confidence bands in quantitative risk analysis, while Spurrier (1999), Bhargava and Spurrier (2004), and Liu *et al.* (2004, 2007) used confidence bands for simultaneous comparisons of several linear regression models in some medical problems.

We will focus on the three most frequently quoted confidence bands in the statistics literature: hyperbolic bands, three-segment bands, and two-segment bands. All the two-sided bands are symmetric about the estimated regression line $\hat{b}_0 + \hat{b}_1 x$ and have the form

$$l(x) = \hat{b}_0 + \hat{b}_1 x - \hat{\sigma} H(x), \quad u(x) = \hat{b}_0 + \hat{b}_1 x + \hat{\sigma} H(x)$$

where $\hat{\sigma} H(x) > 0$ is the half width of the band at x and $H(x)$ determines its shape. One can also construct upper one-sided confidence bands with $l(x) = -\infty$, or lower one-sided confidence bands with $u(x) = \infty$. Denote $\mathbf{d} = (c, d)^T$ and

$$v(c, d) = v(\mathbf{d}) = \mathrm{Var}\{\mathbf{d}^T\ \hat{\boldsymbol{b}}\}/\sigma^2 = \mathbf{d}^T (X^T X)^{-1} \mathbf{d}.$$

Let $\mathbf{x} = (1, x)^T$. A two-sided hyperbolic band has

$$H_{h,2}(x) = c_{h,2} \sqrt{v(\mathbf{x})} \tag{2}$$

where the critical constant $c_{h,2}$ is chosen so that the confidence level is equal to $1-\alpha$. This band for $(a, A) = (-\infty, \infty)$ was proposed by Working and Hotelling (1929) for the special case of known σ while Scheffé (1953, 1959) generalized the Working and Hotelling band to the multiple linear regression model and to unknown σ. When (a, A) is a finite interval, methods of computing $c_{h,2}$ were given by Wynn and Bloomfield (1971) and Uusipaikka (1983). A one-sided hyperbolic band has

$$H_{h,1}(x) = c_{h,1}\sqrt{v(\mathbf{x})} \tag{3}$$

where the critical constant $c_{h,1}$ is chosen so that the confidence level is equal to $1-\alpha$. This one-sided band was considered by Bohrer and Francis (1972) and Pan *et al.* (2003). The shapes of the two-sided and lower one-sided hyperbolic confidence bands are illustrated in Figures 1a and 1b respectively.

Figures 1a and 1b here

A two-sided three-segment band has

$$H_{3,2}(x) = \frac{1}{A-a}\left\{(x-a)c_{3,2,1}\sqrt{v(\boldsymbol{A})} + (A-x)c_{3,2,2}\sqrt{v(\boldsymbol{a})}\right\}, \quad x \in (a, A) \tag{4}$$

where $\boldsymbol{a} = (1, a)^T$, $\boldsymbol{A} = (1, A)^T$, and the two critical constants $c_{3,2,1}$ and $c_{3,2,2}$ are chosen so that the confidence level is equal to $1-\alpha$. This band was proposed by Bowden and Graybill (1966). Notice that this two-sided three-segment band is constructed by putting the following two-sided bounds on the regression line at both $x = a$ and $x = A$

$$b_0 + b_1 a \in \hat{b}_0 + \hat{b}_1 a \pm \hat{\sigma} c_{3,2,2}\sqrt{v(\boldsymbol{a})}, \quad b_0 + b_1 A \in \hat{b}_0 + \hat{b}_1 A \pm \hat{\sigma} c_{3,2,1}\sqrt{v(\boldsymbol{A})}. \tag{5}$$

For x outside of (a, A) the bands are formed of straight lines corresponding to the diagonal elements of the band region within (a, A), so that the upper and lower parts of the band both consist of three line segments. (Although we focus on three linear segments here, diagonal linear extensions can be applied to any band form. See Piegorsch, 1985, for other uses of diagonal band extensions.) When $c_{3,2,2}\sqrt{v(\boldsymbol{a})} = c_{3,2,1}\sqrt{v(\boldsymbol{A})}$, the three-segment band becomes a constant width band over $x \in (a, A)$ which was first considered by Gafarian (1964). In fact, Gafarian's article was the first to restrict a band's inferences to an interval such as (a,A). As we will see, this simple idea has opened up construction of a broad variety of confidence band forms. A one-sided three-segment band has

$$H_{3,1}(x) = \frac{1}{A-a}\left\{(x-a)c_{3,1,1}\sqrt{v(\boldsymbol{A})} + (A-x)c_{3,1,2}\sqrt{v(\boldsymbol{a})}\right\}, \quad x \in (a, A) \tag{6}$$

where the critical constants $c_{3,1,1}$ and $c_{3,1,2}$ are chosen so that the confidence level is equal to $1-\alpha$. The shapes of the two-sided and lower one-sided three-segment confidence bands are illustrated in Figures 2a and 2b respectively.

Figures 2a and 2b here

A two-sided two-segment band is defined over the whole range $(a, A) = (-\infty, \infty)$ and has

$$H_{2,2}(x) = c_{2,2,1}\sqrt{v(\bar{\mathbf{x}})} + c_{2,2,2}|x - \bar{x}|\sqrt{v(\boldsymbol{e})}, \quad x \in (-\infty, \infty) \tag{7}$$

where $\bar{\mathbf{x}} = (1, \bar{x})^T$, $\boldsymbol{e} = (0, 1)^T$, and the critical constants $c_{2,2,1}$ and $c_{2,2,2}$ are chosen so that the confidence level in (1) with $a = -\infty$ and $A = \infty$ is equal to $1-\alpha$. The special case $c_{2,2,1} = c_{2,2,2}$ of this band was first considered by Graybill and Bowden (1967). Notice that this two-sided two-segment band is constructed by putting the following two-sided bounds on the regression line at $x = \bar{x}$ and on the gradient of the regression line b_1

$$b_0 + b_1\bar{x} \in \hat{b}_0 + \hat{b}_1\bar{x} \pm \hat{\sigma}c_{2,2,1}\sqrt{v(\bar{\mathbf{x}})}, \quad b_1 \in \hat{b}_1 \pm \hat{\sigma}c_{2,2,2}\sqrt{v(\boldsymbol{e})}. \tag{8}$$

A one-sided two-segment band is also defined over the whole range $(a, A) = (-\infty, \infty)$ and has

$$H_{2,1}(x) = c_{2,1,1}\sqrt{v(\bar{\mathbf{x}})} + c_{2,1,2}|x - \bar{x}|\sqrt{v(\boldsymbol{e})}, \quad x \in (-\infty, \infty) \tag{9}$$

where the critical constants $c_{2,1,1}$ and $c_{2,1,2}$ are chosen so that the confidence level in (1) with $a = -\infty$ and $A = \infty$ is equal to $1-\alpha$. The shapes of the two-sided and lower one-sided two-segment confidence bands are illustrated in Figures 3a and 3b respectively.

Figures 3a and 3b here

In this paper we derive expression(s) of the simultaneous confidence level, i.e. the left side of equation (1), for each of the confidence bands listed above for given critical constant(s). These expressions can be used to calculate the required critical constants to achieve the preassigned $1-\alpha$ simultaneous confidence level.

For each of these confidence bands, the probability in (1) is in fact independent of b_0, b_1 and σ and so the infimum in (1) can be ignored. The corresponding lower and upper one-sided bands use the same critical constant(s) and so only the lower one-sided confidence bands will be dealt with below. Note that, when $1-\alpha > 0.5$, each critical constant is larger than the t critical value of the $1-\alpha$ one-sided t confidence interval and so is positive. In the rest of the paper, it is assumed that all the critical constants are positive.

2 Preliminaries

Let U be a symmetric positive definite matrix satisfying $(X^T X)^{-1} = U^2$; U is used in the derivations but not the final formulae of the simultaneous confidence level. Note that

$$v(\mathbf{d}) = \mathrm{Var}\{\mathbf{d}^T\ \hat{\boldsymbol{b}}\}/\sigma^2 = \mathbf{d}^T(X^T X)^{-1}\mathbf{d} = \{U\mathbf{d}\}^T\{U\mathbf{d}\} = \|U\mathbf{d}\|^2. \tag{10}$$

Since $\hat{\boldsymbol{b}} \sim N_2(\mathbf{b}, \sigma^2(X^T X)^{-1})$, it is clear that

$$\boldsymbol{N} := U^{-1}(\ \hat{\boldsymbol{b}} - \mathbf{b})/\sigma \ \sim\ N_2(\mathbf{0}, I).$$

Furthermore, since $\hat{\sigma}/\sigma \sim \sqrt{\chi^2_k/k}$ and $\hat{\boldsymbol{b}}$ are independent random variables it follows immediately that

$$\boldsymbol{T} := \boldsymbol{N}/(\hat{\sigma}/\sigma) = U^{-1}(\ \hat{\boldsymbol{b}} - \mathbf{b})/\hat{\sigma} \tag{11}$$

has a standard bivariate t distribution (see e.g. Tong, 1990) whose probability density function (pdf) is given by

$$f_{\boldsymbol{T}}(t_1, t_2) = \frac{1}{2\pi}\left[1 + \frac{1}{k}(t_1^2 + t_2^2)\right]^{-(2+k)/2}, \quad (t_1, t_2) \in R^2.$$

Define the polar coordinates of $\boldsymbol{N} = (N_1, N_2)^T$, $(R_{\boldsymbol{N}}, \theta_{\boldsymbol{N}})$, by

$$N_1 = R_{\boldsymbol{N}} \cos\theta_{\boldsymbol{N}}, \quad N_2 = R_{\boldsymbol{N}} \sin\theta_{\boldsymbol{N}} \text{ for } R_{\boldsymbol{N}} \geq 0 \text{ and } \theta_{\boldsymbol{N}} \in [0, 2\pi).$$

It is well known that $R_{\boldsymbol{N}}$ has the distribution $\sqrt{\chi_2^2}$, $\theta_{\boldsymbol{N}}$ has a uniform distribution on the interval $[0, 2\pi)$, and $R_{\boldsymbol{N}}$ and $\theta_{\boldsymbol{N}}$ are independent. It is clear that the polar coordinates of $\boldsymbol{T}$, $(R_{\boldsymbol{T}}, \theta_{\boldsymbol{T}})$, are given by

$$R_{\boldsymbol{T}} = \|\boldsymbol{T}\| = R_{\boldsymbol{N}}/(\hat{\sigma}/\sigma), \quad \theta_{\boldsymbol{T}} = \theta_{\boldsymbol{N}}$$

and so $R_{\boldsymbol{T}}$ has the distribution $\sqrt{2F_{2,k}}$ where F_{k_1,k_2} denotes an F random variable with degrees of freedom k_1 and k_2, $\theta_{\boldsymbol{T}}$ has a uniform distribution on the interval $[0, 2\pi)$, and $R_{\boldsymbol{T}}$ and $\theta_{\boldsymbol{T}}$ are independent. Straightforward calculation shows that the cumulative distribution function (cdf) of $R_{\boldsymbol{T}}$ is given explicitly by

$$F_{R_{\boldsymbol{T}}}(x) = 1 - (1 + x^2/k)^{-k/2}, \quad x > 0. \tag{12}$$

For a given vector $\boldsymbol{v} \in R^2$ and number $r > 0$, the set

$$\{\boldsymbol{T} : \boldsymbol{v}^T\boldsymbol{T}/\|\boldsymbol{v}\| < r\} \subset R^2 \tag{13}$$

is made up of all the points that are on the same side of the straight line $\boldsymbol{v}^T\boldsymbol{T}/\|\boldsymbol{v}\| = r$ as the origin; the straight line $\boldsymbol{v}^T\boldsymbol{T}/\|\boldsymbol{v}\| = r$ is perpendicular to the vector $\boldsymbol{v}$ and distance r away, in the direction of $\boldsymbol{v}$, from the origin. It follows that the set

$$\{\boldsymbol{T} : |\boldsymbol{v}^T\boldsymbol{T}|/\|\boldsymbol{v}\| < r\} \subset R^2 \tag{14}$$

is simply the strip bounded by the parallel straight lines $\boldsymbol{v}^T\boldsymbol{T}/\|\boldsymbol{v}\| = r$ and $\boldsymbol{v}^T\boldsymbol{T}/\|\boldsymbol{v}\| = -r$.

3 Hyperbolic bands

3.1 Two-sided band

For the two-sided hyperbolic band with $H_{h,2}(x)$ given in (2), the simultaneous confidence level is given by

$$\begin{aligned} & \mathrm{P}\{b_0 + b_1 x \in \hat{b}_0 + \hat{b}_1 x \pm c_{h,2}\hat{\sigma}\sqrt{v(\mathbf{x})} \;\text{ for all } x \in (a, A)\} \\ = \;& \mathrm{P}\left\{ \sup_{x\in(a,A)} |\mathbf{x}^T(\hat{\boldsymbol{b}} - \mathbf{b})/\hat{\sigma}|/\sqrt{v(\mathbf{x})} < c_{h,2} \right\} \\ = \;& \mathrm{P}\left\{ \sup_{x\in(a,A)} \left|\{U\mathbf{x}\}^T \boldsymbol{T}\right| / \|U\mathbf{x}\| < c_{h,2} \right\} = \mathrm{P}\left\{\boldsymbol{T} \in R_{h,2}\right\} \end{aligned} \tag{15}$$

where the first equality in (15) follows from the definition of $\boldsymbol{T}$ in (11) and expression (10). The set $R_{h,2} \subset R^2$ in (15) is given by $R_{h,2} = \cap_{x\in(a,A)} R_{h,2}(x)$ where

$$R_{h,2}(x) = \left\{\boldsymbol{T} : \; \left|\{U\mathbf{x}\}^T \boldsymbol{T}\right| / \|U\mathbf{x}\| < c_{h,2}\right\}.$$

Note that $R_{h,2}(x)$ is of the form (14) and so $R_{h,2}$ is given by the spindle region depicted in Figure 4a. In particular the angle ϕ depicted in the figure is formed by the vectors $U\boldsymbol{a}$ and $U\boldsymbol{A}$, and can be calculated from

$$\cos\phi \;=\; \boldsymbol{a}^T(X^TX)^{-1}\boldsymbol{A}/\sqrt{v(\boldsymbol{a})v(\boldsymbol{A})}. \tag{16}$$

It is worth noting that $\cos\phi$ is simply the correlation coefficient between $\hat{b}_0 + \hat{b}_1 a$ and $\hat{b}_0 + \hat{b}_1 A$.

Figures 4a and 4b here

Note that the probability of $\boldsymbol{T}$ in any region that results from rotating $R_{h,2}$ around the origin is equal to the probability of $\boldsymbol{T}$ in $R_{h,2}$ since the pdf of $\boldsymbol{T}$ is rotationally invariant. In particular, let $R^*_{h,2}$ be the region that results from rotating $R_{h,2}$ around the origin so that the angle ϕ is divided into two equal halves by the t_2-axis, as depicted in Figure 4b. This region $R^*_{h,2}$ has the expression

$$R^*_{h,2} = \{\boldsymbol{T} : \; |\boldsymbol{v}^T\boldsymbol{T}|/\|\boldsymbol{v}\| < c_{h,2} \;\text{ for all } \boldsymbol{v} \in E(\phi)\}$$

where $E(\phi) = \{\boldsymbol{v} = (v_1, v_2)^T : \ v_2 > \|\boldsymbol{v}\| \cos(\phi/2)\}$ is a cone. Hence the simultaneous confidence level is equal to

$$\mathrm{P}\left\{\boldsymbol{T} \in R_{h,2}\right\} = \mathrm{P}\left\{\boldsymbol{T} \in R^*_{h,2}\right\} = \mathrm{P}\left\{\sup_{\boldsymbol{v} \in E(\phi)} |\boldsymbol{v}^T \boldsymbol{T}|/\|\boldsymbol{v}\| < c_{h,2}\right\}. \tag{17}$$

Next we derive three expressions for this simultaneous confidence level.

3.1.1 The method of Wynn and Bloomfield (1971)

This method was given by Wynn and Bloomfield (1971) and calculates the probability $\mathrm{P}\{\boldsymbol{T} \in R^*_{h,2}\}$ directly. Note that $R^*_{h,2}$ can be partitioned into the whole disc of radius $c_{h,2}$ and the remaining region. The probability of $\boldsymbol{T}$ in the disc is given by

$$\mathrm{P}\{\|\boldsymbol{T}\| < c_{h,2}\} = \mathrm{P}\{R_{\boldsymbol{T}} < c_{h,2}\} = 1 - \left(1 + c^2_{h,2}/k\right)^{-k/2} \tag{18}$$

where the last equality follows immediately from the cdf of $R_{\boldsymbol{T}}$ in (12). The probability of $\boldsymbol{T}$ in the remaining region is equal to four times the probability of $\boldsymbol{T}$ in the cross-line shaded region in Figure 4b and so given by

$$\begin{aligned}
& 4\mathrm{P}\{\ \theta_{\boldsymbol{T}} \in [0, (\pi-\phi)/2],\ \|\boldsymbol{T}\| > c_{h,2},\ (\cos[(\pi-\phi)/2], \sin[(\pi-\phi)/2])\boldsymbol{T} < c_{h,2}\ \} \\
= \ & 4\mathrm{P}\{\ 0 < \theta_{\boldsymbol{T}} < (\pi-\phi)/2,\ c_{h,2} < R_{\boldsymbol{T}} < c_{h,2}/\cos[(\pi-\phi)/2 - \theta_{\boldsymbol{T}}]\ \} \qquad (19) \\
= \ & 4\int_0^{(\pi-\phi)/2} \frac{1}{2\pi} \mathrm{P}\{\ c_{h,2} < R_{\boldsymbol{T}} < c_{h,2}/\cos[(\pi-\phi)/2 - \theta]\ \} d\theta \\
= \ & \frac{2}{\pi}\int_0^{(\pi-\phi)/2} \left\{ \left[1 + \frac{c^2_{h,2}}{k}\right]^{-k/2} - \left[1 + \frac{c^2_{h,2}}{k\sin^2(\theta+\phi/2)}\right]^{-k/2} \right\} d\theta \qquad (20)
\end{aligned}$$

where equality (19) follows directly by representing $\boldsymbol{T}$ in the polar coordinates. Combining expressions (18) and (20) gives the simultaneous confidence level as

$$1 - \frac{\phi}{\pi}\left[1 + \frac{c^2_{h,2}}{k}\right]^{-k/2} - \frac{2}{\pi}\int_0^{(\pi-\phi)/2} \left[1 + \frac{c^2_{h,2}}{k\sin^2(\theta+\phi/2)}\right]^{-k/2} d\theta. \tag{21}$$

3.1.2 An algebraic method

This method evaluates

$$\mathrm{P}\left\{\sup_{\boldsymbol{v}\in E(\phi)} |\boldsymbol{v}^T\boldsymbol{T}|/\|\boldsymbol{v}\| < c_{h,2}\right\} = \mathrm{P}\left\{\|\boldsymbol{T}\| \sup_{\boldsymbol{v}\in E(\phi)} |\boldsymbol{v}^T\boldsymbol{T}|/(\|\boldsymbol{v}\|\|\boldsymbol{T}\|) < c_{h,2}\right\} \tag{22}$$

by finding an explicit expression for the supremum. The approach is similar to that of Casella and Strawderman (1980).

Note that $\boldsymbol{v}^T\boldsymbol{T}/(\|\boldsymbol{v}\|\|\boldsymbol{T}\|)$ is equal to the cosine of the angle between $\boldsymbol{T}$ and $\boldsymbol{v}$, and $\cos\theta$ is monotone decreasing in $\theta \in [0, \pi]$. So the supremum is attained at the vector $\boldsymbol{v} \in E(\phi) \cup -E(\phi)$ that forms the smallest angle with $\boldsymbol{T}$. From this geometric reasoning it is clear that

$$\sup_{\boldsymbol{v}\in E(\phi)} \frac{|\boldsymbol{v}^T\boldsymbol{T}|}{\|\boldsymbol{v}\|} = \begin{cases} \|\boldsymbol{T}\| & \text{if } \theta_{\boldsymbol{T}} \in [(\pi-\phi)/2, (\pi+\phi)/2] \cup [(3\pi-\phi)/2, (3\pi+\phi)/2], \\ \|\boldsymbol{T}\||\sin(\theta_{\boldsymbol{T}}+\phi/2)| & \text{if } \theta_{\boldsymbol{T}} \in [0, (\pi-\phi)/2] \cup [\pi, (3\pi-\phi)/2], \\ \|\boldsymbol{T}\||\sin(\theta_{\boldsymbol{T}}-\phi/2)| & \text{if } \theta_{\boldsymbol{T}} \in [(\pi+\phi)/2, \pi] \cup [(3\pi+\phi)/2, 2\pi). \end{cases}$$

The simultaneous confidence level (22) is therefore equal to

$$\begin{aligned} & \mathrm{P}\{\ \theta_{\boldsymbol{T}} \in [(\pi-\phi)/2, (\pi+\phi)/2] \cup [(3\pi-\phi)/2, (3\pi+\phi)/2],\quad \|\boldsymbol{T}\| < c_{h,2}\ \} \\ + & \mathrm{P}\{\ \theta_{\boldsymbol{T}} \in [0, (\pi-\phi)/2] \cup [\pi, (3\pi-\phi)/2],\quad \|\boldsymbol{T}\||\sin(\theta_{\boldsymbol{T}}+\phi/2)| < c_{h,2}\ \} \\ + & \mathrm{P}\{\ \theta_{\boldsymbol{T}} \in [(\pi+\phi)/2, \pi] \cup [(3\pi+\phi)/2, 2\pi],\quad \|\boldsymbol{T}\||\sin(\theta_{\boldsymbol{T}}-\phi/2)| < c_{h,2}\ \} \\ = & \frac{2\phi}{2\pi}\mathrm{P}\{\ \|\boldsymbol{T}\| < c_{h,2}\ \} \\ + & 2\int_0^{(\pi-\phi)/2} \frac{1}{2\pi}\mathrm{P}\{\ \|\boldsymbol{T}\||\sin(\theta+\phi/2)| < c_{h,2}\ \}\, d\theta \qquad (23) \\ + & 2\int_{(\pi+\phi)/2}^{\pi} \frac{1}{2\pi}\mathrm{P}\{\ \|\boldsymbol{T}\||\sin(\theta-\phi/2)| < c_{h,2}\ \}\, d\theta \qquad (24) \\ = & \frac{\phi}{\pi}\mathrm{P}\{\ R_{\boldsymbol{T}} < c_{h,2}\ \} \qquad (25) \\ + & \frac{2}{\pi}\int_0^{(\pi-\phi)/2} \mathrm{P}\{\ R_{\boldsymbol{T}} < c_{h,2}/|\sin(\theta+\phi/2)|\ \}\, d\theta \\ = & \frac{\phi}{\pi}\left[1-\left(1+\frac{c_{h,2}^2}{k}\right)^{-k/2}\right] + \frac{2}{\pi}\int_0^{(\pi-\phi)/2}\left[1-\left(1+\frac{c_{h,2}^2}{k\sin^2(\theta+\phi/2)}\right)^{-k/2}\right] d\theta \qquad (26) \end{aligned}$$

where equality (25) follows by observing that the two integrals in (23) and (24) are equal, and equality (26) follows from the cdf of $R_{\boldsymbol{T}}$. It is clear that expression (26) is equal to expression (21).

3.1.3 The method of Uusipaikka (1983)

This method was given by Uusipaikka (1983) and hinges on the volume of tubular neighborhoods of $E(\phi)$. Due to the simplicity of the cone $E(\phi)$, the exact volume of tubular neighborhoods of $E(\phi)$ can be easily calculated. The idea of this method has been further developed by many authors (e.g. Naiman, 1986 and 1990). From (17), the simultaneous confidence level is given by

$$
\begin{aligned}
& 1 - \mathrm{P}\left\{ \sup_{\boldsymbol{v}\in E(\phi)} \frac{|\boldsymbol{v}^T\boldsymbol{T}|}{\|\boldsymbol{v}\|\|\boldsymbol{T}\|} \geq \frac{c_{h,2}}{\|\boldsymbol{T}\|} \right\} \\
= \ & 1 - \int_0^\infty \mathrm{P}\left\{ \sup_{\boldsymbol{v}\in E(\phi)} \frac{|\boldsymbol{v}^T\boldsymbol{T}|}{\|\boldsymbol{v}\|\|\boldsymbol{T}\|} \geq \frac{c_{h,2}}{w} \right\} dF_{R_{\boldsymbol{T}}}(w) \qquad (27) \\
= \ & 1 - \int_{c_{h,2}}^\infty \mathrm{P}\left\{ \sup_{\boldsymbol{v}\in E(\phi)} \frac{|\boldsymbol{v}^T\boldsymbol{T}|}{\|\boldsymbol{v}\|\|\boldsymbol{T}\|} \geq \frac{c_{h,2}}{w} \right\} dF_{R_{\boldsymbol{T}}}(w) \qquad (28)
\end{aligned}
$$

where (27) is due to the independence of $R_{\boldsymbol{T}}$ and $\theta_{\boldsymbol{T}}$ since the supremum depends on $\boldsymbol{T}$ only through $\theta_{\boldsymbol{T}}$ (see below), and (28) follows directly from the fact that the supremum is no larger than one. The probability in (28) can be written as $\mathrm{P}\{\theta_{\boldsymbol{T}} \in |E|(\phi, c_{h,2}/w)\}$ where, for $0 < r < 1$,

$$
\begin{aligned}
|E|(\phi, r) &= \left\{ \boldsymbol{T} : \sup_{\boldsymbol{v}\in E(\phi)} \frac{|\boldsymbol{v}^T\boldsymbol{T}|}{\|\boldsymbol{v}\|\|\boldsymbol{T}\|} \geq r \right\} \\
&= \left\{ \theta_{\boldsymbol{T}} : \sup_{\boldsymbol{v}\in E(\phi)} |\cos(\theta_{\boldsymbol{T}} - \theta_{\boldsymbol{v}})| \geq \cos(\arccos r) \right\}.
\end{aligned}
$$

Figure 5 here

$|E|(\phi, r)$ refers to the tubular neighborhoods of $E(\phi) \cup -E(\phi)$ of angular radius $\arccos r$, and is depicted in Figure 5. It is clear from the definition and Figure 5 that $|E|(\phi, r)$ can further be expressed as

$$
|E|(\phi, r) = \left\{ \theta_{\boldsymbol{T}} \in \left[\frac{\pi - \phi}{2} - \arccos r, \frac{\pi + \phi}{2} + \arccos r \right] \cup \left[\frac{3\pi - \phi}{2} - \arccos r, \frac{3\pi + \phi}{2} + \arccos r \right] \right\}
$$

when $\phi/2 + \arccos r < \pi/2$ and

$$
|E|(\phi, r) = \{\theta_{\boldsymbol{T}} \in [0, 2\pi]\}
$$

when $\phi/2 + \arccos r \geq \pi/2$. Note that

$$\phi/2 + \arccos(c_{h,2}/w) < \pi/2 \Longleftrightarrow w < c_{h,2}/\sin(\phi/2)$$

and $\theta_{\boldsymbol{T}}$ has a uniform distribution on $[0, 2\pi)$. We therefore have, for $c_{h,2} \leq w < c_{h,2}/\sin(\phi/2)$,

$$\mathrm{P}\{\theta_{\boldsymbol{T}} \in |E|(\phi, c_{h,2}/w)\} = [2\arccos(c_{h,2}/w) + \phi]/\pi \tag{29}$$

and, for $w \geq c_{h,2}/\sin(\phi/2)$,

$$\mathrm{P}\{\theta_{\boldsymbol{T}} \in |E|(\phi, c_{h,2}/w)\} = 1. \tag{30}$$

Substituting (29) and (30) into (28) gives the confidence level as

$$\begin{aligned} & 1 - \int_{c_{h,2}}^{c_{h,2}/\sin(\phi/2)} \frac{2\arccos(c_{h,2}/w) + \phi}{\pi} dF_{R_{\boldsymbol{T}}}(w) - \int_{c_{h,2}/\sin(\phi/2)}^{\infty} 1 dF_{R_{\boldsymbol{T}}}(w) \\ = \quad & 1 - \left(1 + \frac{c_{h,2}^2}{k\sin^2(\phi/2)}\right)^{-k/2} - \int_{c_{h,2}}^{c_{h,2}/\sin(\phi/2)} \frac{2\arccos(c_{h,2}/w) + \phi}{\pi} dF_{R_{\boldsymbol{T}}}(w). \end{aligned} \tag{31}$$

Both expressions (26) and (31) involve one-dimensional integrations and can be used to compute the simultaneous confidence level. It can be shown that the two expressions are equal as expected.

For the special case of $(a, A) = (-\infty, \infty)$, the angle $\phi = \pi$. From expressions (18) or (25) the simultaneous confidence level becomes $\mathrm{P}\{R_{\boldsymbol{T}} < c_{h,2}\} = \mathrm{P}\{F_{2,k} < c_{h,2}^2/2\}$ and so $c_{h,2} = \sqrt{2 f_{2,k}^{\alpha}}$, where $f_{2,k}^{\alpha}$ is the upper α-point of the $F_{2,k}$ distribution.

3.2 One-sided band

For the lower one-sided hyperbolic band with $H_{h,1}(x)$ given in (3), the simultaneous confidence level is given by

$$\mathrm{P}\left\{\sup_{x \in (a,A)} [\mathbf{x}^T(\hat{\boldsymbol{b}} - \mathbf{b})/\hat{\sigma}]/\sqrt{v(\mathbf{x})} < c_{h,1}\right\} = \mathrm{P}\left\{\boldsymbol{T} \in R_{h,1}\right\} \tag{32}$$

where the set $R_{h,1} \subset R^2$ in (32) is given by $R_{h,1} = \cap_{x \in (a,A)} R_{h,1}(x)$ with

$$R_{h,1}(x) = \left\{\boldsymbol{T} : \left[\{U\mathbf{x}\}^T \boldsymbol{T}\right] / \|U\mathbf{x}\| < c_{h,1}\right\}.$$

Note that $R_{h,1}(x)$ is of the form (13).

Rotate $R_{h,1}$ around the origin, in a similar way to rotating $R_{h,2}$ in the two-sided case, to $R^*_{h,1}$ as depicted in Figure 6; the angle ϕ is the same as in the two-sided case and divided into two equal halves by the t_2-axis. This region $R^*_{h,1}$ has the expression

$$R^*_{h,1} = \{\boldsymbol{T} : \ \boldsymbol{v}^T\boldsymbol{T}/\|\boldsymbol{v}\| < c_{h,2} \ \text{ for all } \boldsymbol{v} \in E(\phi)\}$$

where $E(\phi)$ is the same as in the two-sided case. Due to the rotational invariance of the $\boldsymbol{T}$ probability distribution, the simultaneous confidence level is further equal to

$$\mathrm{P}\left\{\boldsymbol{T} \in R^*_{h,1}\right\} = \mathrm{P}\left\{\sup_{\boldsymbol{v}\in E(\phi)} \boldsymbol{v}^T\boldsymbol{T}/\|\boldsymbol{v}\| < c_{h,1}\right\}. \tag{33}$$

We next derive three expressions for this simultaneous confidence level.

Figure 6 here

3.2.1 The method of Bohrer and Francis (1972)

Bohrer and Francis (1972) calculate the probability $\mathrm{P}\{\boldsymbol{T} \in R^*_{h,1}\}$ directly. Note that $R^*_{h,1}$ can be partitioned into four parts as depicted in Figure 6: the fan C_1, the cone C_2, and the two half-strips C_3 and C_4. The probability of $\boldsymbol{T}$ in C_1 is equal to

$$\mathrm{P}\left\{ \ \theta_{\boldsymbol{T}} \in [(\pi-\phi)/2, (\pi+\phi)/2], \ \|\boldsymbol{T}\| \le c_{h,1} \ \right\} = \frac{\phi}{2\pi}\mathrm{P}\left\{ \ \|\boldsymbol{T}\| \le c_{h,1} \ \right\} = \frac{\phi}{2\pi}F_{2,k}\left(\frac{c^2_{h,1}}{2}\right). \tag{34}$$

The probability of $\boldsymbol{T}$ in C_2 is given by

$$\mathrm{P}\left\{ \ \theta_{\boldsymbol{T}} \in [(3\pi-(\pi-\phi))/2, (3\pi+(\pi-\phi))/2] \ \right\} = \frac{\pi-\phi}{2\pi}. \tag{35}$$

Again due to the rotational invariance of the $\boldsymbol{T}$ probability distribution, the probability of $\boldsymbol{T}$ in $C_3 \cup C_4$ is equal to the probability of $\boldsymbol{T}$ in the strip which is the union of C_4 and the half-strip that results from rotating C_3 clockwise at angle ϕ, and further equal to the probability of $\boldsymbol{T}$ in the strip that results from rotating the last strip clockwise at angle $(\pi-\phi)/2$:

$$\mathrm{P}\{ \ 0 < T_1 < c_{h,1} \ \} = \frac{1}{2}F_{1,k}(c^2_{h,1}). \tag{36}$$

Collecting (34), (35) and (36) together gives the simultaneous confidence level as

$$\frac{\pi-\phi}{2\pi}+\frac{1}{2}F_{1,k}(c_{h,1}^2)+\frac{\phi}{2\pi}F_{2,k}\left(\frac{c_{h,1}^2}{2}\right). \tag{37}$$

3.2.2 An algebraic method

This method is similar to that for the two-sided case in Section 3.1.2; the key is to find an explicit expression for the supremum in (33), which is given by

$$\sup_{\boldsymbol{v}\in E(\phi)}\frac{\boldsymbol{v}^T\boldsymbol{T}}{\|\boldsymbol{v}\|}=\begin{cases}\|\boldsymbol{T}\| & \text{if } \theta_{\boldsymbol{T}}\in[(\pi-\phi)/2,(\pi+\phi)/2],\\ \|\boldsymbol{T}\|\cos[(\pi-\phi)/2-\theta_{\mathbf{T}}] & \text{if } \theta_{\boldsymbol{T}}\in[-\pi/2,(\pi-\phi)/2],\\ \|\boldsymbol{T}\|\cos[\theta_{\boldsymbol{T}}-(\pi+\phi)/2] & \text{if } \theta_{\boldsymbol{T}}\in[(\pi+\phi)/2,3\pi/2].\end{cases}$$

Note in particular that the supremum is negative when $\theta_{\boldsymbol{T}}\in(-\pi/2,(\pi-\phi)/2-\pi/2)\cup((\pi+\phi)/2+\pi/2,3\pi/2)$ and that $c_{h,1}>0$. A derivation similar to the two-sided case gives the simultaneous confidence level (33) equal to

$$\frac{\phi}{2\pi}F_{R_{\boldsymbol{T}}}(c_{h,1})+\frac{\pi-\phi}{2\pi}+\frac{1}{\pi}\int_0^{\pi/2}F_{R_{\boldsymbol{T}}}\left(\frac{c_{h,1}}{\cos(\theta)}\right)d\theta. \tag{38}$$

3.2.3 The method of Uusipaikka

Uusipaikka's (1983) method of Section 3.1.3 was manipulated by Pan, Piegorsh and West (2003) to also provide one-sided bounds. From (33), the simultaneous confidence level is given by

$$1-\int_{c_{h,1}}^{\infty}\mathrm{P}\left\{\sup_{\boldsymbol{v}\in E(\phi)}\frac{\boldsymbol{v}^T\boldsymbol{T}}{\|\boldsymbol{v}\|\|\boldsymbol{T}\|}\geq\frac{c_{h,1}}{w}\right\}dF_{R_{\boldsymbol{T}}}(w).$$

A derivation similar to the two-sided case in Section 3.1.3 shows that the probability in the last expression is equal to $[2\arccos(c_{h,1}/w)+\phi]/[2\pi]$ and so the confidence level is given by

$$1-\int_{c_{h,1}}^{\infty}\frac{2\arccos(c_{h,1}/w)+\phi}{2\pi}dF_{R_{\boldsymbol{T}}}(w). \tag{39}$$

It is straightforward to show that expressions (39), (38) and (37) are equal, as expected. But of course expression (37) is the simplest to use as it involves only the cdf's of $F_{1,k}$ and $F_{2,k}$. When

$(a, A) = (-\infty, \infty)$, the angle $\phi = \pi$. In this case expression (37) simplifies to

$$\frac{1}{2}F_{1,k}(c_{h,1}^2) + \frac{1}{2}F_{2,k}\left(\frac{c_{h,1}^2}{2}\right),$$

which agrees with the result of Hochberg and Quade (1975).

4 Three-segment bands

4.1 Two-sided band

For the two-sided three-segment band with $H_{3,2}(x)$ given in (4), the simultaneous confidence level is given by

$$\mathrm{P}\left\{\sup_{x\in(a,A)} |\mathbf{x}^T(\hat{\boldsymbol{b}} - \mathbf{b})/\hat{\sigma}|/H_{3,2}(x) < 1\right\}. \tag{40}$$

Note that

$$\frac{\partial}{\partial x}\left\{[\mathbf{x}^T(\hat{\boldsymbol{b}} - \mathbf{b})/\hat{\sigma}]/H_{3,2}(x)\right\}$$

has a fixed sign, either positive or negative, over $x \in (-\infty, \infty)$. The supremum in (40) is therefore attained at either $x = a$ or $x = A$, and so the confidence level can further be expressed as

$$\mathrm{P}\left\{\max_{x=a \text{ or } A} |\mathbf{x}^T(\hat{\boldsymbol{b}} - \mathbf{b})/\hat{\sigma}|/H_{3,2}(x) < 1\right\} = \mathrm{P}\left\{\boldsymbol{T} \in R_{3,2}\right\}$$

where $R_{3,2} = R_{3,2}(a) \cap R_{3,2}(A)$ with

$$R_{3,2}(a) \quad = \quad \left\{\boldsymbol{T}:\ |\boldsymbol{a}^T(\hat{\boldsymbol{b}} - \mathbf{b})/\hat{\sigma}|/H_{3,2}(a) < 1\ \right\} = \left\{\boldsymbol{T}:\ \left|\{U\boldsymbol{a}\}^T\boldsymbol{T}\right| / \|U\boldsymbol{a}\| < c_{3,2,2}\right\}$$

and, in a similar fashion,

$$R_{3,2}(A) = \left\{\boldsymbol{T}:\ \left|\{U\boldsymbol{A}\}^T\boldsymbol{T}\right| / \|U\boldsymbol{A}\| < c_{3,2,1}\right\}.$$

Note that both $R_{3,2}(a)$ and $R_{3,2}(A)$ are of the form (14). Hence $R_{3,2}$ is given by the parallelogram depicted in Figure 7a. In particular the angle ϕ depicted in the picture is formed by the vectors

$U\boldsymbol{a}$ and $U\boldsymbol{A}$ as in the hyperbolic bands. It is noteworthy that $R_{3,2}$ can actually be derived from the two constraints in (5).

Figures 7a and 7b here

Let $R^*_{3,2}$ be the region that results from rotating $R_{3,2}$ around the origin so that $U\boldsymbol{A}$ is in the direction of the t_1-axis, as depicted in Figure 7b. Hence the confidence level is equal to the probability of $\boldsymbol{T}$ in $R^*_{3,2}$ and further equal to twice the probability of $\boldsymbol{T}$ in the portion of $R^*_{3,2}$ to the right of the dotted line which has the expression

$$\{\boldsymbol{T}:\ \theta_{\boldsymbol{T}} \in [-(\pi-\eta_1),\xi_1], R_{\boldsymbol{T}}\cos\theta_{\boldsymbol{T}} \le c_{3,2,1}\} \cup \{\boldsymbol{T}:\ \theta_{\boldsymbol{T}} \in [\xi_1,\eta_1], R_{\boldsymbol{T}}\cos(\theta_{\boldsymbol{T}}-\phi) \le c_{3,2,2}\}$$

where the angles ξ_1 and η_1 are depicted in Figure 7b and given by

$$\xi_1 = \arcsin\left(\frac{c_{3,2,2}-c_{3,2,1}\cos\phi}{\sqrt{c_{3,2,2}^2+c_{3,2,1}^2-2c_{3,2,2}c_{3,2,1}\cos\phi}}\right), \tag{41}$$

$$\eta_1 = \arccos\left(\frac{-c_{3,2,1}\sin\phi}{\sqrt{c_{3,2,2}^2+c_{3,2,1}^2+2c_{3,2,2}c_{3,2,1}\cos\phi}}\right). \tag{42}$$

These two expressions can be found by first determining the (t_1,t_2)-equations of the four straight lines that form the parallelogram $R^*_{3,2}$, then solving the (t_1,t_2)-coordinates of the four vertices of $R^*_{3,2}$ and finally converting the (t_1,t_2)-coordinates into polar coordinates.

Hence the simultaneous confidence level is equal to

$$\begin{aligned}
& 2\mathrm{P}\left\{\theta_{\boldsymbol{T}} \in [-(\pi-\eta_1),\xi_1], R_{\boldsymbol{T}}\cos\theta_{\boldsymbol{T}} \le c_{3,2,1}\right\} + 2\mathrm{P}\left\{\theta_{\boldsymbol{T}} \in [\xi_1,\eta_1], R_{\boldsymbol{T}}\cos(\theta_{\boldsymbol{T}}-\phi) \le c_{3,2,2}\right\} \\
= \ & 2\int_{-(\pi-\eta_1)}^{\xi_1} \frac{1}{2\pi}\mathrm{P}\left\{R_{\boldsymbol{T}}\cos\theta \le c_{3,2,1}\right\} d\theta + 2\int_{\xi_1}^{\eta_1} \frac{1}{2\pi}\mathrm{P}\left\{R_{\boldsymbol{T}}\cos(\theta-\phi) \le c_{3,2,2}\right\} d\theta \\
= \ & \frac{1}{\pi}\int_{-(\pi-\eta_1)}^{\xi_1} F_{R_{\boldsymbol{T}}}\left(\frac{c_{3,2,1}}{\cos\theta}\right) d\theta + \frac{1}{\pi}\int_{\xi_1-\phi}^{\eta_1-\phi} F_{R_{\boldsymbol{T}}}\left(\frac{c_{3,2,2}}{\cos\theta}\right) d\theta.
\end{aligned} \tag{43}$$

Expression (43) involves only one-dimensional integration since $F_{R_{\boldsymbol{T}}}(\cdot)$ is given explicitly in (12). Bowden and Graybill (1966) expressed the simultaneous confidence level as a two-dimensional integral of a bivariate t density function. In the special case of a constant width band, i.e. $c_{3,2,1}\sqrt{v(\boldsymbol{A})} = c_{3,2,2}\sqrt{v(\boldsymbol{a})}$, Gafarian (1964) expressed the simultaneous confidence level as a one-dimensional integral similar to (43) by using polar coordinates.

4.2 One-sided band

For the lower one-sided three-segment band with $H_{3,1}(x)$ given in (6), the simultaneous confidence level is given by

$$\mathrm{P}\left\{ \max_{x=a \text{ or } A} [\mathbf{x}^T(\hat{\boldsymbol{b}} - \mathbf{b})/\hat{\sigma}]/H_{3,1}(x) < 1 \right\} = \mathrm{P}\{\boldsymbol{T} \in R_{3,1}\}$$

where $R_{3,1} = R_{3,1}(a) \cap R_{3,1}(A)$ with

$$R_{3,1}(a) = \left\{ \boldsymbol{T} : \left[\{U\boldsymbol{a}\}^T \boldsymbol{T} \right] / \|U\boldsymbol{a}\| < c_{3,1,2} \right\}$$

and

$$R_{3,1}(A) = \left\{ \boldsymbol{T} : \left[\{U\boldsymbol{A}\}^T \boldsymbol{T} \right] / \|U\boldsymbol{A}\| < c_{3,1,1} \right\}.$$

Note that both $R_{3,1}(a)$ and $R_{3,1}(A)$ are of the form (13).

Rotate $R_{3,1}$ around the origin, in a similar way to rotating $R_{3,2}$ in the two-sided case, to $R_{3,1}^*$ so that $U\boldsymbol{A}$ is in the direction of the t_1-axis. Thus the confidence level is equal to the probability of $\boldsymbol{T}$ in $R_{3,1}^*$ and has the following expression after a few lines of simple calculation

$$\frac{1}{2\pi} \int_{\xi_2 - \phi}^{\pi/2} F_{R_{\boldsymbol{T}}} \left(\frac{c_{3,1,2}}{\cos\theta} \right) d\theta + \frac{1}{2\pi} \int_{-\pi/2}^{\xi_2} F_{R_{\boldsymbol{T}}} \left(\frac{c_{3,1,1}}{\cos\theta} \right) d\theta + \frac{\pi - \phi}{2\pi},$$

where the angle ξ_2 corresponds to the angle ξ_1 in the two-sided case and is given by

$$\xi_2 = \arcsin\left(\frac{c_{3,1,2} - c_{3,1,1}\cos\phi}{\sqrt{c_{3,1,2}^2 + c_{3,1,1}^2 - 2c_{3,1,2}c_{3,1,1}\cos\phi}} \right),$$

and the angle ϕ is the same as in the two-sided case.

In practice, the values of a and A are chosen by the needs of the investigator. If the values of a and A are such that $\hat{b}_0 + \hat{b}_1 a$ and $\hat{b}_0 + \hat{b}_1 A$ are independent random variables then $\phi = \pi/2$ from (16) and all the simultaneous confidence expressions in Sections 3 and 4 can be simplified to certain extent as shown in Hayter, Liu and Wynn (2007).

5 Two-segment bands

5.1 Two-sided band

For the two-sided two-segment band with $H_{2,2}(x)$ given in (7), the simultaneous confidence level is given by

$$\mathrm{P}\left\{\sup_{x\in(-\infty,\infty)} |\mathbf{x}^T(\hat{\boldsymbol{b}}-\mathbf{b})/\hat{\sigma}|/H_{2,2}(x)<1\right\}. \tag{44}$$

Note that

$$\frac{\partial}{\partial x}\left\{[\mathbf{x}^T(\hat{\boldsymbol{b}}-\mathbf{b})/\hat{\sigma}]/H_{2,2}(x)\right\}$$

has a fixed sign, either positive or negative, over $x>\bar{x}$ and over $x<\bar{x}$. The supremum in (44) is therefore attained at either $x=\bar{x}$ or limits $x\to-\infty$ or $x\to\infty$. As a result, the confidence level can further be expressed as

$$\mathrm{P}\left\{\sup_{x=-\infty \text{ or } \bar{x} \text{ or } \infty} |\mathbf{x}^T(\hat{\boldsymbol{b}}-\mathbf{b})/\hat{\sigma}|/H_{2,2}(x)<1\right\}=\mathrm{P}\left\{\boldsymbol{T}\in R_{2,2}\right\}$$

where $R_{2,2}=R_{2,2}(-\infty)\cap R_{2,2}(\bar{x})\cap R_{2,2}(\infty)$ with

$$R_{2,2}(\bar{x}) = \left\{\boldsymbol{T}:\ |\bar{\mathbf{x}}^T(\hat{\boldsymbol{b}}-\mathbf{b})/\hat{\sigma}|/H_{2,2}(\bar{x})<1\right\}=\left\{\boldsymbol{T}:\ \left|\{U\bar{\mathbf{x}}\}^T\boldsymbol{T}\right|/\|U\bar{\mathbf{x}}\|<c_{2,2,1}\right\},$$

and

$$R_{2,2}(\pm\infty) = \left\{\boldsymbol{T}:\ \lim_{x\to\infty}|\mathbf{x}^T(\hat{\boldsymbol{b}}-\mathbf{b})/\hat{\sigma}|/H_{2,2}(x)<1\right\}=\left\{\boldsymbol{T}:\ \left|\{U\boldsymbol{e}\}^T\boldsymbol{T}\right|/\|U\boldsymbol{e}\|<c_{2,2,2}\right\}.$$

Note that $R_{2,2}(\bar{x})$ and $R_{2,2}(\pm\infty)$ are of the form (14). Hence $R_{2,2}$ is given by the parallelogram depicted in Figure 8. In particular the angle $\phi^*\in(0,\pi)$ depicted in the picture is formed by the vectors $U\boldsymbol{e}$ and $U\bar{\mathbf{x}}$ and can be calculated to be $\phi^*=\pi/2$ since $\cos\phi^*=0$. It is noteworthy that $R_{2,2}$ can actually be derived from the two constraints in (8).

Figure 8 here

By comparing the parallelogram $R_{2,2}$ in Figure 8 with the parallelogram $R_{3,2}$ for the two-sided three-segment band in Figure 7a, the confidence level $\mathrm{P}\{\boldsymbol{T}\in R_{2,2}\}$ is given by expression (43) but with $c_{3,2,1}, c_{3,2,2}, \phi$ replaced with $c_{2,2,1}, c_{2,2,2}, \phi^* = \pi/2$ respectively, i.e.

$$\mathrm{P}\{\boldsymbol{T} \in R_{2,2}\} = \frac{1}{\pi}\int_{-(\pi-\eta_1^*)}^{\xi_1^*} F_{R_{\boldsymbol{T}}}\left(\frac{c_{2,2,1}}{\cos\theta}\right) d\theta + \frac{1}{\pi}\int_{\xi_1^*-\phi^*}^{\eta_1^*-\phi^*} F_{R_{\boldsymbol{T}}}\left(\frac{c_{2,2,2}}{\cos\theta}\right) d\theta \tag{45}$$

where

$$\xi_1^* = \arcsin\left(\frac{c_{2,2,2}}{\sqrt{c_{2,2,2}^2 + c_{2,2,1}^2}}\right), \quad \eta_1^* = \arccos\left(\frac{-c_{2,2,1}}{\sqrt{c_{2,2,2}^2 + c_{2,2,1}^2}}\right).$$

Note that the angles ξ_1^* and η_1^* correspond to the angles ξ_1 in (41) and η_1 in (42) respectively.

For the special case of $c_{2,2,2} = c_{2,2,1}$, Graybill and Bowden (1967) expressed the simultaneous confidence level as a two-dimensional integral of a bivariate t density function. Expression (45) involves only one-dimensional integration, however.

5.2 One-sided band

The lower one-sided two-segment band has $H_{2,1}(x)$ given in (9). Similar to the two-sided case, the simultaneous confidence level is given by $\mathrm{P}\left\{\boldsymbol{T} \in R_{2,1}\right\}$where $R_{2,1} = R_{2,1}(-\infty) \cap R_{2,1}(\bar{x}) \cap R_{2,1}(\infty)$ with

$$R_{2,1}(\bar{x}) = \left\{\boldsymbol{T} : \{U\bar{\mathbf{x}}\}^T \boldsymbol{T} / \|U\bar{\mathbf{x}}\| < c_{2,1,1}\right\},$$

$$R_{2,1}(\infty) = \left\{\boldsymbol{T} : \{U\boldsymbol{e}\}^T \boldsymbol{T} / \|U\boldsymbol{e}\| < c_{2,1,2}\right\},$$

and

$$R_{2,1}(-\infty) = \left\{\boldsymbol{T} : \{U\boldsymbol{e}\}^T \boldsymbol{T} / \|U\boldsymbol{e}\| > -c_{2,1,2}\right\}.$$

Note that $R_{2,1}(\bar{x})$ is of the form (13) and $R_{2,1}(\infty) \cap R_{2,1}(-\infty)$ is of the form (14).

Let $R_{2,1}^*$ be the region that results from rotating $R_{2,1}$ around the origin so that $U\bar{\mathbf{x}}$ is in the direction of the t_1-axis. Hence the confidence level is equal to the probability of $\boldsymbol{T}$ in $R_{2,1}^*$ and has the following expression after a few lines of calculation similar to before:

$$\frac{1}{2\pi}\int_{-(\pi-\eta_2^*)}^{\xi_2^*} F_{R_{\boldsymbol{T}}}\left(\frac{c_{2,1,1}}{\cos\theta}\right) d\theta + \frac{1}{2\pi}\int_{\xi_2^*-\phi^*}^{\pi/2} F_{R_{\boldsymbol{T}}}\left(\frac{c_{2,1,2}}{\cos\theta}\right) d\theta + \frac{1}{2\pi}\int_{\pi/2}^{\eta_2^*+\pi-\phi^*} F_{R_{\boldsymbol{T}}}\left(\frac{-c_{2,1,2}}{\cos\theta}\right) d\theta,$$

where the angles ξ_2^* and η_2^* correspond to the angles ξ_1 and η_1 in Figure 7b respectively and are given by

$$\xi_2^* = \arcsin\left(\frac{c_{2,1,2}}{\sqrt{c_{2,1,2}^2 + c_{2,1,1}^2}}\right) \quad \text{and} \quad \eta_2^* = \arccos\left(\frac{-c_{2,1,1}}{\sqrt{c_{2,1,2}^2 + c_{2,1,1}^2}}\right).$$

6 Concluding remarks

We have described expressions for calculating simultaneous confidence levels associated with two-sided and one-sided hyperbolic, three-segment, and two-segment confidence bands. The results are exact for the special, but nonetheless ubiquitous, case of simple linear regression with homoscedastic normal errors. These expressions involve one-dimensional integration in general, except for the one-sided hyperbolic band whose simultaneous confidence level can be expressed to involve only the cdf's of the $F_{1,k}$ and $F_{2,k}$ distributions.

The key idea in deriving these expressions is to express the simultaneous confidence level as the probability of the bivariate vector $\boldsymbol{T}$ from (11) in a region $R \subset R^2$. Note that the region R can always be represented using the polar coordinates $(R_{\boldsymbol{T}}, \theta_{\boldsymbol{T}})$ in the form

$$R = \{\boldsymbol{T} : \ \theta_{\boldsymbol{T}} \in [\theta_1, \theta_2], R_{\boldsymbol{T}} \le G(\theta_{\boldsymbol{T}})\}$$

for some given constants $0 \le \theta_1 \le \theta_2 \le 2\pi$ and given function G. So the simultaneous confidence level is given by

$$\int_{\theta_1}^{\theta_2} \frac{1}{2\pi} F_{R_{\boldsymbol{T}}}[G(\theta)]d\theta$$

since $\theta_{\boldsymbol{T}}$ is uniformly distributed on the interval $[0, 2\pi)$ and independent of $R_{\boldsymbol{T}}$ whose cdf $F_{R_{\boldsymbol{T}}}(\cdot)$ is given in (12).

By inverting these expressions for the simultaneous confidence level, one can calculate the critical constant(s) necessary to achieve a required confidence level. Note, however, that two critical constants are employed in both the three-segment band and in the two-segment band. So, an additional constraint above and beyond the $1-\alpha$ specification is required to determine the two critical constants uniquely. Gafarian (1966) imposed $c_{3,2,1}\sqrt{v(\boldsymbol{A})} = c_{3,2,2}\sqrt{v(\boldsymbol{a})}$ and Graybill and Bowden (1967) imposed $c_{2,2,1} = c_{2,2,2}$. This extra constraint may also be based on certain optimality criteria, such as the average width optimality considered by Naiman (1983, 1984) and Piegorsch (1985) among others, or the minimum area confidence set optimality considered by Liu and Hayter (2007). Of course, the average width or minimum area confidence set optimality can be used to compare two confidence bands and/or to identify the optimal confidence band.

There are other less well known confidence bands. For example, Bowden (1970) showed how the two-sided hyperbolic, three-segment and two-segment bands and a general p-family confidence bands can be derived from Hölder's inequality. Piegorsch *et al.* (2000) used polar coordinates as used in this paper and a bivariate t distribution to compute the simultaneous confidence level of the p-family confidence bands with

$$H_p(x) = (1 + \tau|x|^p)^{1/p}$$

where $\tau > 0$ and $p \geq 1$ are given constants. Other confidence bands include those given by Naiman (1984, 1987a) which are optimal under certain criteria.

Confidence bands for multiple linear regression models are much harder to construct. Some notable works include Knafl, Sacks and Ylvisaker (1985), Naiman (1987b, 1990), Sun and Loader (1994), Sun, Loader and McCormick (2000) and Liu *et al.* (2005) for the situation that the explanatory variables are constrained to a hyper-rectangle, and Bohrer (1973), Casella and Strawderman (1980), and Seppanen and Uusipaikka (1992) for the situation that the explanatory variables are constrained to a hyper-ellipsoid.

Acknowledgements: We would like to thank the Associate Editor and referees for several constructive comments.

References

Al-Saidy, O.M., Piegorsch, W.W., West, R.W. and Nitcheva, D.K. (2003). Confidence bands for low-dose risk estimation with quantal response data. *Biometrics*, 59, 1056-1062.

Bhargava, P. and Spurrier, J.D. (2004). Exact confidence bands for comparing two regression lines with a control regression line on a fixed interval. *Biometrical Journal*, 46, 720-730.

Bohrer, R. (1973). A multivariate t probability integral. *Biometrika*, 60, 647-654.

Bohrer, R. and Francis, G.K. (1972). Sharp one-sided confidence bands for linear regression over intervals. *Biometrika*, 59, 99-107.

Bowden, D.C. and Graybill, F.A. (1966). Confidence bands of uniform and proportional width for linear models. *J. Amer. Stat. Assoc.*, 61, 182-198.

Bowden, D.C. (1970). Simultaneous confidence bands for linear regression models. *J. Amer. Stat. Assoc.*, 65, 413-421.

Casella, G. and Strawderman, W.E. (1980). Confidence bands for linear-regression with restricted predictor variables. *J. Amer. Stat. Assoc.*, 75, 862-868.

Gafarian, A.V. (1964). Confidence bands in straight line regression. *J. Amer. Stat. Assoc.*, 59, 182-213.

Graybill, F. A. and Bowden, D. C. (1967). Linear Segment Confidence Bands for Simple Linear Regression Models. *J. Amer. Stat. Assoc.*, 62, 403-408.

Hayter, A.J., Liu, W. and Wynn, H.P. (2007). Easy-to-Construct Confidence Bands for Comparing Two Simple Linear Regression Lines. *J. of Statistical Planning and Inferences*, 137(4), 1213-1225.

Hochberg, Y. and Quade, D. (1975). One-sided simultaneous confidence bounds on regression surfaces with intercepts. *J. Amer. Stat. Assoc.*, 70, 889-891.

Knafl, G., Sacks, J. and Ylvisaker, D. (1985). Confidence bands for regression-func -tions. *J. Amer. Stat. Assoc.*, 80, 683-691.

Liu, W. and Hayter, A.J. (2007). Minimum area confidence set optimality for confidence bands in simple linear regression. *J. Amer. Stat. Assoc.*, 102(477), 181-190.

Liu, W., Jamshidian, M., Zhang, Y. (2004) Multiple comparison of several regression models. *J. Amer. Stat. Assoc.*, 99, 395-403.

Liu, W., Jamshidian, M., Zhang, Y. and Donnelly, J. (2005). Simulation-based simultaneous confidence bands for a multiple linear regression model when the covariates are constrained. *J. of Computational and Graphical Statistics*, 14(2), 459-484.

Liu, W., Jamshidian, M., Zhang, Y., Bretz, F. and Han, X. (2007). Pooling batches in drug stability study by using constant width simultaneous confidence bands. *Statistics in Medicine*, 26(14), 2759-2771.

Naiman, D.Q. (1983). Comparing Scheffé-type to constant-width confidence bands in regression. *J. Amer. Stat. Assoc.*, 78, 906-912.

Naiman, D.Q. (1986). Conservative confidence bands in curvilinear regression. *Ann. Statist.*, 14, 896-906.

Naiman, D.Q. (1987a). Minimax regret simultaneous confidence bands for multiple regression functions. *J. Amer. Stat. Assoc.*, 82, 894-901.

Naiman, D.Q. (1987b). Simultaneous confidence-bounds in multiple-regression using predictor variable constraints. *J. Amer. Stat. Assoc.*, 82, 214-219.

Naiman, D.Q. (1990). On volumes of tubular neighborhoods of spherical polyhedra and statistical inference. *Ann. Statist.*, 18, 685-716.

Pan, W., Piegorsch, W.W. and West, R.W. (2003). Exact one-sided simultaneous confidence bands via Uusipaikka's method. *Annals of the Institute of Statistical Mathematics*, 55 (2), 243-250.

Piegorsch, W.W. (1985). Admissible and optimal confidence bands in simple linear-regression. *Ann. Stat.*, 13. 810-810.

Piegorsch, W.W. (1985). Average-width optimality for confidence bands in simple linear-regression. *J. Amer. Stat. Assoc.*, 80. 692-697.

Piegorsch, W.W., West R.W., Al-Saidy O.M. and Bradley, K.D. (2000). Asymmetric confidence bands for simple linear regression over bounded intervals. *Computational Statistics & Data Analysis*, 34(2), 193-217.

Piegorsch, W.W., West R.W., Pan, W. and Kodell, R. (2005). Low dose risk estimation via simultaneous statistical inferences. *J. Roy. Stat. Soc. C*, 245-258.

Scheffé, H. (1953). A method for judging all contrasts in analysis of variance. *Biometrika*, 40, 87-104

Scheffé, H. (1959). *The Analysis of Variance.* Wiley.

Seppanen, E. and Uusipaikka, E. (1992). Confidence bands for linear-regression over restricted regions. *Scand. J. Stat.*, 19, 73-81.

Spurrier, J.D. (1999). Exact Confidence Bounds for All Contrasts of Three or More Regression Lines. *J. Amer. Stat. Assoc.*, 94, 483-88.

Sun, J. and Loader, C.R. (1994.) Simultaneous confidence bands for linear regression and smoothing. *Ann. Statist.*, 22, 1328-1346.

Sun,J., Loader, C.R. and McCormick, W.P. (2000). Confidence bands in generalized linear models. *Ann. Statist.*, 28, 429-460.

Sun,J., Raz, J. and Faraway, J.J. (1999). Simultaneous confidence bands for growth and response curves. *Statistica Sinica*, 9(3), 679-698.

Tong, Y.L. (1990). *Multivariate Normal Distribution.* Springer-Verlag.

Uusipaikka, E. (1983). Exact confidence bands for linear-regression over intervals. *J. Amer. Stat. Assoc.*, 78, 638-644.

Working, H. and Hotelling, H. (1929). Applications of the theory of error to the interpretation of trends. *J. Amer. Stat. Assoc.*, 24, 73-85.

Wynn, H.P. and Bloomfield, P. (1971). Simultaneous confidence bands in regression analysis. *J. Roy. Stat. Soc. B*, 33, 202-217

Figure 1a: two-sided hyperbolic band

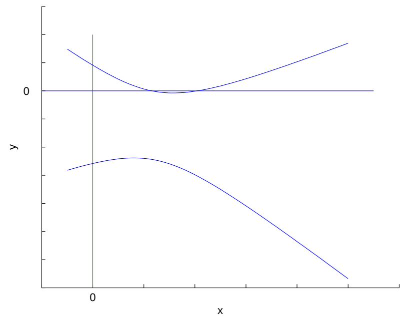

Figure 1b: lower one-sided hyperbolic band

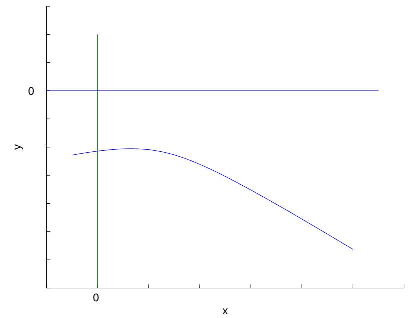

Figure 2a: two-sided 3-segment band

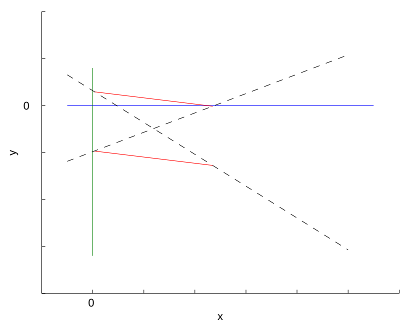

Figure 2b: lower one-sided 3-segment band

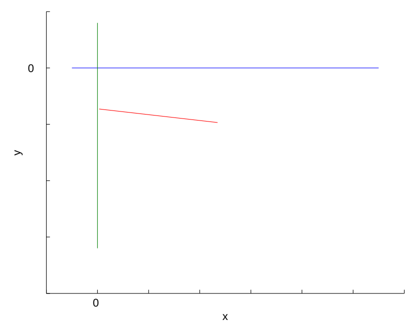

Figure 3a: two-sided 2-segment band

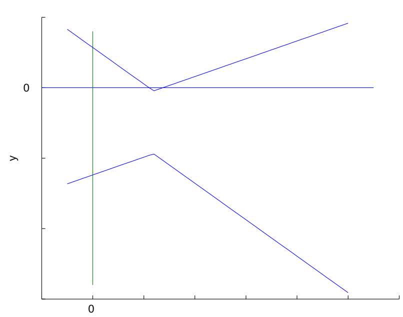

Figure 3b: lower one-sided 2-segment band

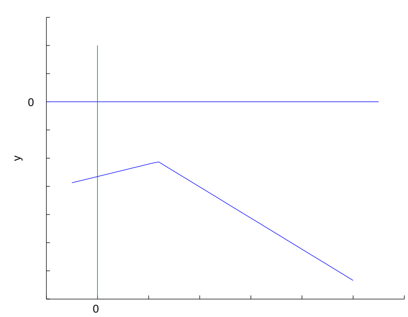

Figure 4a: the region $R_{h,2}$

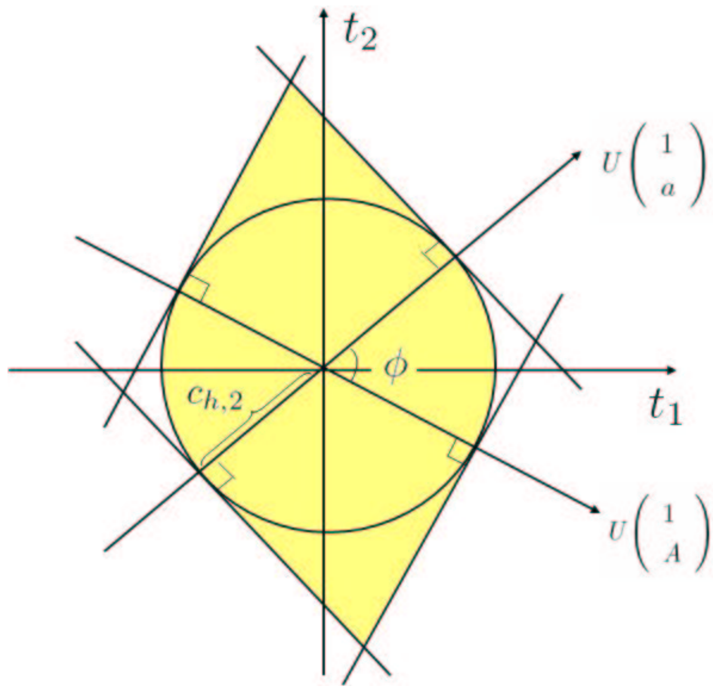

Figure 4b: the region $R^*_{h,2}$

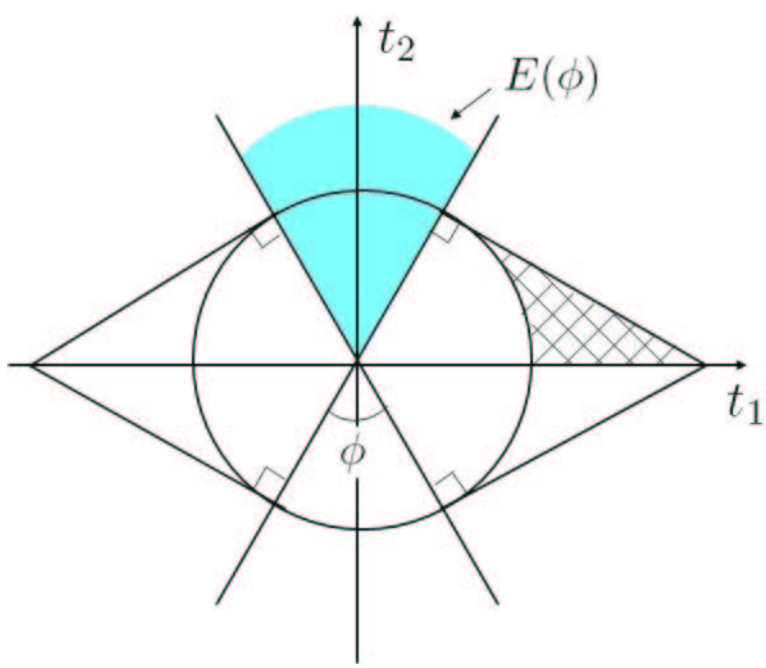

Figure 5: the region $|E|(\phi, r)$

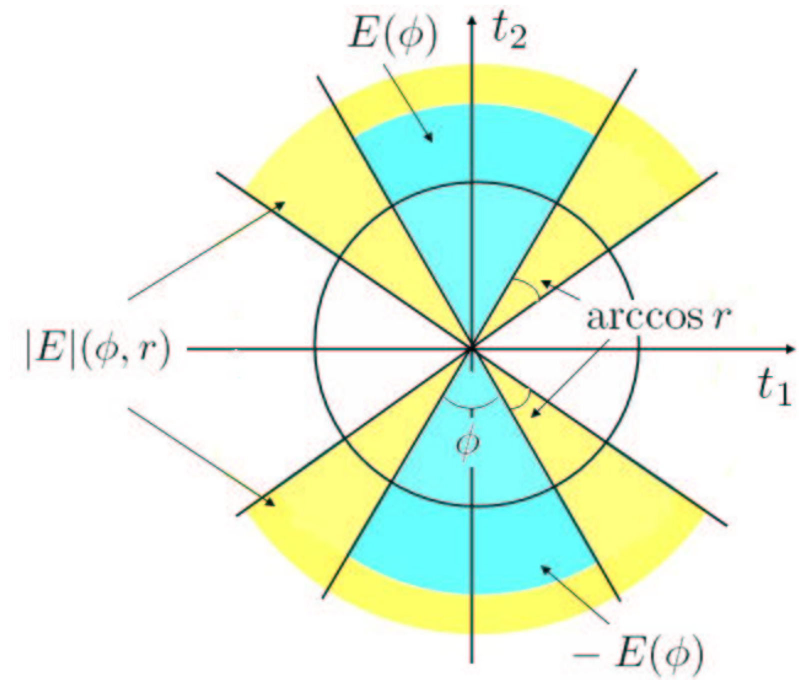

Figure 6: the region $R^*_{h,1}$

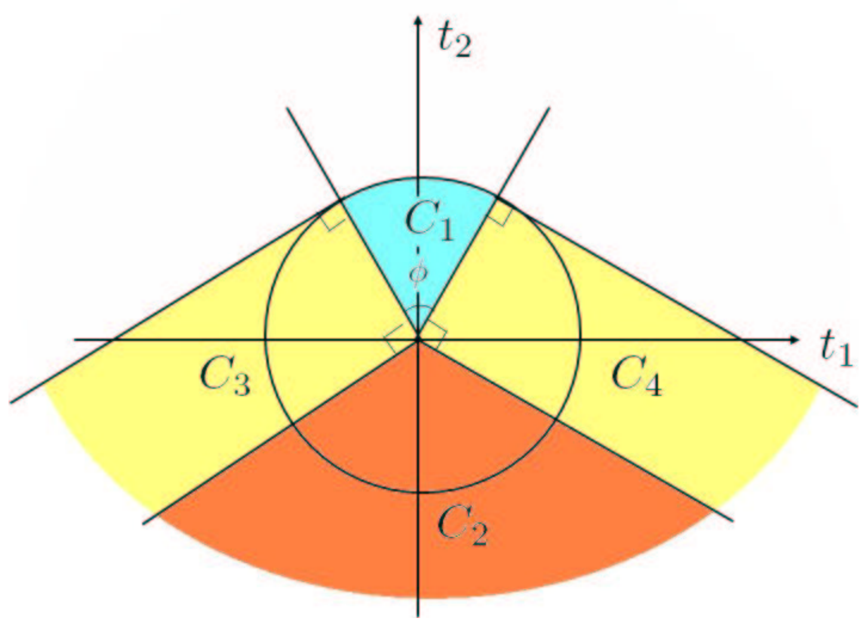

Figure 7a: the region $R_{3,2}$

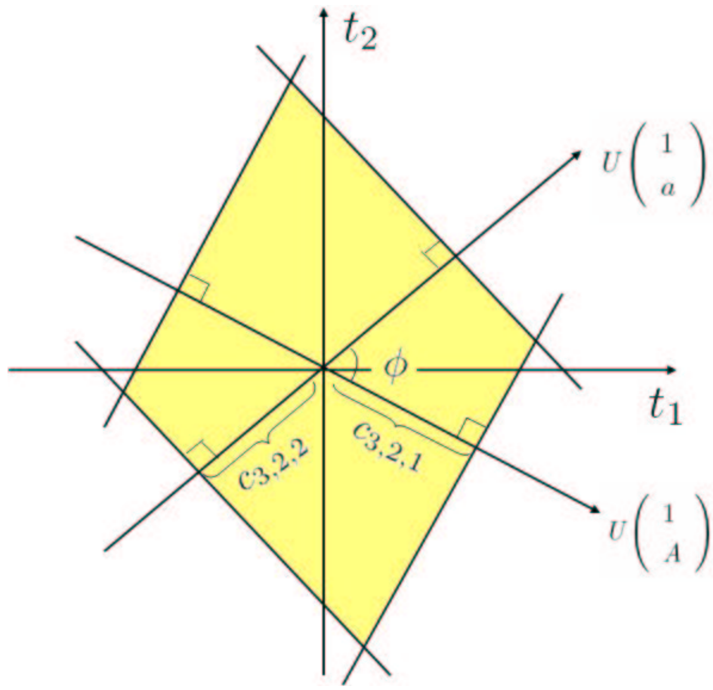

Figure 7b: the region $R^*_{3,2}$

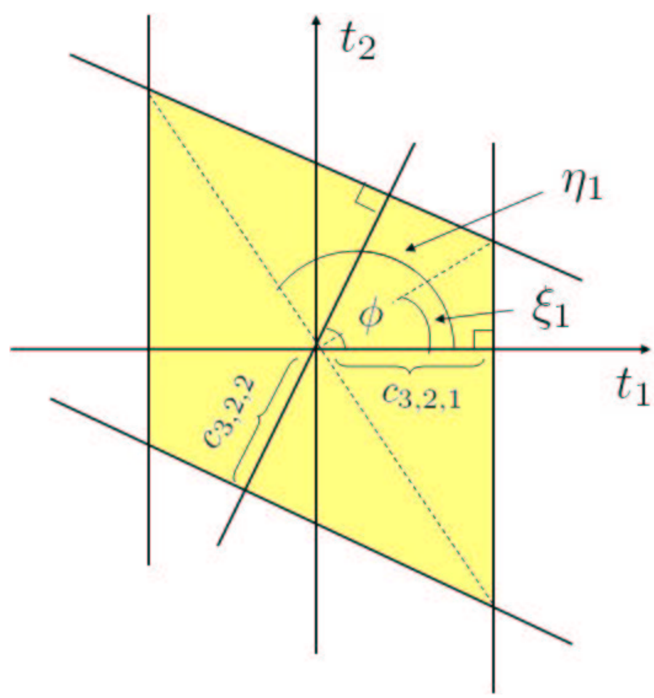

Figure 8: the region $R_{2,2}$